BIOLOGY OF REPRODUCTION **72,** 293–300 (2005)
Published online before print 8 September 2004.
DOI 10.1095/biolreprod.104.033092

Clonal Organization of Proliferating Spermatogonial Stem Cells in Adult Males of Two Species of Non-Human Primates, *Macaca mulatta* and *Callithrix jacchus*[1]

Jens Ehmcke,[3] Craig Marc Luetjens,[4] and Stefan Schlatt[2,3,4]

Department of Cell Biology and Physiology,[3] Center for Research in Reproductive Physiology, University of Pittsburgh School of Medicine, Pittsburgh, Pennsylvania 15261
Institute of Reproductive Medicine,[4] University Münster, 48149 Münster, Germany

ABSTRACT

The present study examines the existence of clonogenic patterns in the proliferation and differentiation of spermatogonial stem cells in two species of non-human primates, the marmoset and the rhesus monkey. We developed a novel approach to detect proliferating spermatogonial clones in whole mounts of seminiferous tubules. Dual fluorescence labeling of bromodeoxyuridine and acrosin in conjunction with confocal microscopy allows the description of the clonogenic and spatial arrangement of proliferating spermatogonia at specific stages of the seminiferous epithelial cycle. Cross-sections of paraffin-embedded tissue were labeled by the same approach. For both monkey species we demonstrate the presence of proliferating spermatogonial clones of variable size at specific stages of the cycle of the seminiferous epithelium. Detailed analysis of the rhesus monkey reveals proliferating A_{pale} spermatogonia at stages VII and IX of the cycle of the seminiferous epithelium, and of proliferating B spermatogonia at stages II, IV, VI, and XII. Proliferating A_{pale} spermatogonia at stages VII and IX of the cycle are organized in pairs or quadruplets. B_1 spermatogonia appear as quadruplets or eight-cell clones, and B_2 spermatogonia as 8- or 16-cell clones. We conclude that spermatogenesis in the rhesus monkey is initiated by two divisions of duplets or quadruplets of A_{pale} spermatogonia: a first division at stage VII, after which the clones of A_{pale} spermatogonia separate, and a second division at stage IX, which leads to clones of B_1 spermatogonia as well as pairs and quadruplets of A_{pale} spermatogonia replenishing the seminiferous epithelium to maintain the original size of the A spermatogonial population.

gamete biology, spermatogenesis

INTRODUCTION

In the testis of adult mammalian species, spermatogonial stem cells maintain their numbers by self-renewal and give rise to differentiating germ cells. Most of the diploid germ cells are differentiating spermatogonia undergoing several rounds of mitotic divisions before entering meiotic prophase. In non-human primates seven different types of spermatogonia have been identified [1–6]: the reserve stem cell A_{dark} spermatogonium; the renewing stem cell A_{pale} spermatogonium; the intermediate $A_{transition}$ spermatogonium; and four generations of B spermatogonia, B_1, B_2, B_3, and B_4. It has been unequivocally demonstrated that B spermatogonia derive from A_{pale} spermatogonia [1]. However, the complex kinetics and the circumstances of the unequal division of A_{pale} spermatogonia replenishing their own numbers and giving rise to B spermatogonia are poorly understood.

Previous studies have focused on the cycle of the seminiferous epithelium and on the proliferation of spermatogonial stem cells in different species of non-human primates and other mammalian species, leading to several models for spermatogonial expansion and differentiation [1–3, 5, 7–14]. Some of these studies examined whole mount preparations of seminiferous tubules to obtain qualitative data on spermatogonial organization. Most previous studies applied morphometric approaches on (serial) cross-sections of seminiferous tubules, producing valuable data on spermatogonial counts and labeling indices. However, none of the previous studies has so far presented an in-depth evaluation of the proposed [1, 2, 13] clonal organization of spermatogonial stem cells at different stages of spermatogenesis, and some models of the expansion of spermatogonial stem cells contradict each other.

In the adult testis, proliferating spermatogonia and preleptotene spermatocytes in S-phase of meiosis can be detected by nuclear incorporation of Bromodeoxyuridine (BrdU) [15]. We first encountered clones of proliferating spermatogonia in the marmoset (*Callithrix jacchus*) by using a whole mount approach. As the seminiferous epithelium in this species does not present longitudinally separated stages of spermatogenesis, it is difficult to correlate spermatogonial clones with specific stages of spermatogenesis [16]. We therefore continued our studies using the rhesus monkey (*Macaca mulatta*), which shows a longitudinal separation of 12 different stages of the cycle of the seminiferous epithelium.

Criteria for the staging of the macaque seminiferous epithelium had first been established by Clermont and Leblond [1], Clermont [2], and Clermont and Antar [3] based on periodic acid Schiff reagent staining of the acrosome and hematoxylin counterstaining of nuclei. The immunofluorescent localization of acrosin allowed us to accurately determine the size and shape of the acrosome. We used changes of the acrosomal immunostaining to accurately determine the stages of spermatogenesis [1–3]. It was our first aim to correlate our novel staining method on sections and whole mounts of rhesus monkey testicular tissue to the originally described 12 stages of the seminiferous epithelial cycle. We describe well-defined categories enabling us to identify these 12 stages of the spermatogenic cycle both in

[1]Supported by a Heisenberg fellowship (Schl394/3) and a research grant from the Deutsche Forschungsgemeinschaft (Schl394/6), as well as startup funds from the University of Pittsburgh School of Medicine.
[2]Correspondence: Stefan Schlatt, University of Pittsburgh, School of Medicine, Department of Cell Biology and Physiology, W952 Biomedical Science Tower, 3500 Terrace Street, Pittsburgh, PA 15261.
FAX: 412 648 8315; e-mail: schlatt@pitt.edu

Received: 11 June 2004.
First decision: 19 July 2004.
Accepted: 27 August 2004.

ISSN: 0006-3363. http://www.biolreprod.org

whole mounts of seminiferous tubules and on testicular sections using our dual- and triple-label immunohistochemical approach.

We then aimed to analyze and describe the initiating division(s) and the clonogenic expansion of spermatogonia to propose a well-defined model of premeiotic germ cell development in the rhesus monkey.

MATERIALS AND METHODS

Animals

Two adult (one age 2.7 yr, body weight 375 g, and the other 4.1 yr and 350 g, with a testicular weight between 0.3 and 0.5 g) male marmosets (*C. jacchus*) were included in this study. Maintenance, handling, and all surgical procedures of these monkeys were performed in accordance with the German Federal Law on the Care and Use of Laboratory Animals.

Five adult (age 6.2–12 yr, body weight 9.8–13.5 kg, testicular weight 20.9–61.5 g) male rhesus monkeys (*M. mulatta*) were included in this study. The animals where maintained at the University of Pittsburgh Plum Borough Primate Research Facility in accordance with the NIH Guidelines for the Care and Use of Laboratory Animals. One of the monkeys had taken part in previous endocrinological studies, but had been allowed to recover for a period of more than 6 mo before the present study. Three additional monkeys served as control animals in an ongoing study examining the effect of FSH and LH on spermatogenesis. For this purpose, endocrine gonadotropin release was blocked by treatment with a GnrH antagonist (acyline; for details on establishing a chronic hypogonadotropic state in rhesus monkeys using acyline, see [17]), and the restoration of physiologically normal FSH and LH blood levels was attempted using exogenous recombinant human FSH and recombinant human LH. In the control group, all parameters (blood testosterone level, testicular volume, diameter of the seminiferous tubules, thickness and histological appearance of the seminiferous epithelium) indicated that the LH dose was appropriate to establish normal levels of androgens and that the dose of FSH was stimulatory, rather than suppressive. As a consequence, the testis weights were in the upper normal range for rhesus monkeys. All experimental procedures were approved by the University of Pittsburgh Institutional Animal Care and Use Committee.

Surgical Procedures

The marmosets received an intraperitoneal (i.p.) bolus injection of BrdU (100 mg/kg body weight; Sigma-Aldrich, Munich, Germany) 3 h before castration. Four rhesus monkeys received an intravenous (i.v.) bolus of BrdU (33 mg/kg body weight; Sigma, St. Louis, MO) 3 h before castration or hemi-castration. One rhesus monkey received an i.v. bolus injection of BrdU 40 days before the removal of the testis. For surgery the monkeys were first sedated with ketamine hydrochloride: 10 mg/kg body weight for the marmosets (Park-Advise, Munich, Germany) and 10 mg/kg body weight i.m. for the rhesus monkeys (Ketaject, Phoenix Scientific Inc., St. Joseph, MO). The marmosets were then killed by exsanguination and the testes were removed postmortem. The rhesus monkeys were anesthetized with isoflurane in oxygen (1%–2.5%; Abbott Laboratories, North Chicago, IL). All surgical procedures were performed under aseptic conditions. Postsurgically rhesus monkeys received one daily intramuscular injection of penicillin (300 000 U, Bicillin L-A; Wyeth Laboratories, Philadelphia, PA) and an analgesic (1 mg/kg body weight, Meperidine hydrochloride, Demerol; Abbott Laboratories) for 4 days.

Tissue Preparation

For sectioning, testicular tissue samples were fixed overnight at 4°C in Bouin fixative, washed in 70% ethanol, dehydrated, and routinely embedded in paraffin. Five-micrometer serial sections were cut.

For whole mount staining, fresh testes were decapsulated and tissue samples were teased in sterile PBS to obtain fragments of seminiferous tubules, each between several millimeters and 2 cm in length. At this stage, some fragments of testicular tissue retrieved from the macaque that had received an i.v. bolus of BrdU 40 days before castration was incubated for 2 h at 37°C in Dulbecco modified eagle medium (DMEM; 4.5 g glucose/L; Mediatech, Herndon, VA) supplemented with nonessential amino acids (Cambrex Bio Science, Walkerville, MD; dilution following manufacturer's instructions); Glutamin (365 mg/L; Sigma); antibiotics (penicillin 100 IU/ml, streptomycin 100 μg/ml; Mediatech, Herndon, VA); and BrdU (100 μM; Sigma) to allow cells in S-phase to incorporate BrdU. All testicular tubules were fixed overnight at 4°C in Bouin fixative and washed and stored in 70% ethanol.

Conventional Staining Procedure

Sections were deparaffinized, rehydrated, incubated for 15 min at room temperature (RT) in fresh periodic acid solution (1% in distilled water), washed with distilled water, incubated for 15 min in Schiff reagent, washed with distilled water, stained with hematoxylin solution (all reagents from Sigma), washed in tap water followed by distilled water, transferred through rising ethanol concentrations into xylene, and mounted with permanent mounting medium.

Whole mounts were rehydrated, stained with hematoxylin solution, washed with tap water followed by distilled water, and—to avoid shrinkage occurring during dehydration—mounted with VectaShield aqueous mounting medium (Vector, Burlingame, CA).

Immunohistochemical Staining Procedure

Sections of testicular tissue were deparaffinized; rehydrated; incubated in 1M hydrochloric acid for 10 min at RT; washed in distilled water; incubated for 5 min at RT with Trypsin (0.1% in Tris buffered saline [TBS]; Sigma); washed with distilled water followed by TBS; incubated for 30 min at RT with blocking solution (5% goat serum and 0.1% bovine serum albumin [BSA] in TBS; goat serum and BSA from Sigma); and incubated overnight at 4°C with the primary antibody (monoclonal anti-BrdU, clone BU-33 [either from Sigma or Biomeda, Foster City, CA] diluted 1:50 in TBS containing 0.1% BSA). Then the sections were washed with TBS; incubated for 1 h at RT with the secondary antibody (goat–anti-mouse, biotinylated [Sigma], diluted 1:100 in TBS containing 0.1% BSA); washed with TBS; incubated for 1 h at RT with a mix of a second primary antibody and a streptavidin-conjugated fluorescent dye (monoclonal anti-acrosin, clone Acr-C5F10 [Biosonda, Miami, FL], and fluorescent dye AlexaFluor 488, streptavidin-conjugated [Molecular Probes, Eugene, OR], both diluted 1:100 in TBS containing 0.1% BSA); washed in TBS; incubated for 1 h at RT with a secondary antibody (Goat–anti-Mouse, fluorescent dye AlexaFluor 546-conjugated [Molecular Probes], diluted 1:100 in TBS containing 0.1% BSA) washed with TBS and mounted using VectaShield Mounting Medium (Vector) containing 4,6-Diamidino-2-phenylindole (DAPI; 1.5 μg/ml).

For immunohistochemical staining of whole mounts, a similar protocol as described for sections was applied, differing in longer incubation times for hydrochloric acid and trypsin solution (15 min at RT for both in whole mount staining). For the visualization of the BrdU label in some seminiferous tubules of the marmoset, a peroxidase-conjugated secondary antibody (Goat–anti-Mouse, peroxidase-conjugated; Sigma-Aldrich) and DAB-staining (3,3′-diaminobenzidine, peroxidase substrate; Sigma-Aldrich) were used to produce an insoluble brown precipitate in BrdU-positive nuclei. All whole mounts were mounted on microscope slides using VectaShield mounting medium without DAPI (Vector).

Tissue Analysis

Sections and whole mounts were analyzed using a Nikon Eclipse E800 fluorescence microscope (Nikon, Melville, NY) with attached digital camera (Olympus, Melville, NY) and Nikon CI confocal scanning system. All images were acquired digitally using MagnaFire Software (Optronics, Goleta, CA).

Determination of Stages of the Cycle of the Seminiferous Epithelium on Sections and Whole Mounts of Seminiferous Tubules After Immunohistochemistry

When the tissue had been exposed to hydrochloric acid and trypsin to allow access of the antibody to BrdU incorporated into the nuclear DNA, the nuclear counterstaining with DAPI was only intense in the heads of elongated spermatids from step 13 onward (stages I to VI of the cycle of the seminiferous epithelium as defined by Clermont and Leblond [1]). This allowed us to distinguish the following types of spermatids: 1) round spermatids from step 1 to step 7 (stage I to stage VII of the cycle); 2) DAPI-negative elongating spermatids from step 8 to step 12 (corresponds to stage VIII to stage XII of the cycle); 3) DAPI-positive elongated spermatids (from step 13 onward).

The colocalization of BrdU as a proliferation marker, acrosin as a spermatid label, and DAPI as DNA-staining of the most mature spermatids enabled us to identify proliferating cells and to correlate their presence

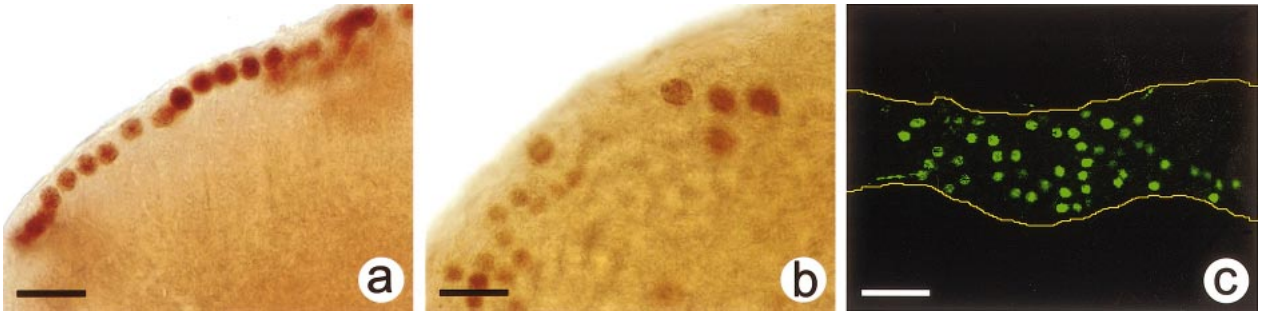

FIG. 1. Immunohistochemical localization of BrdU. Bright field (**a** and **b**) and confocal (**c**) micrographs of whole mounts of adult marmoset testes. **a**) BrdU-positive cells (dark brown DAB-precipitate) in intact seminiferous tubules. These cells form a continuous, longitudinally positioned line adjacent to the basement membrane of the tubule. Bar = 25 μm. **b**) BrdU-positive cells (dark brown DAB-precipitate) in intact seminiferous tubules. Juxtaposed nuclei of two distinctly different sizes can be observed. Bar = 25 μm. **c**) BrdU-positive cells (green fluorescent label) in intact seminiferous tubules (the yellow superimposed lines outline the seminiferous tubule). The BrdU-positive cells are organized in a spatially arranged pattern. Bar = 50 μm.

with accurately determined stages of spermatogenesis depending on acrosomal structure and the presence of one or two types of spermatids. Therefore, we first evaluated criteria to correlate our staining patterns in tissue sections with the morphological criteria used for the determination of stages by Clermont and Leblond [1]. In whole mounts of tissue, the DAPI staining was obsolete as the presence of elongated spermatids in the seminiferous tubules could easily be determined using conventional phase contrast microscopy.

Evaluation of Spermatogonial Clones

In accordance with the definitions used to describe clones of undifferentiated spermatogonia in rodents [18, 19] and cohorts of monkey spermatogonia [1–3], we defined cohorts of neighbored BrdU-positive spermatogonia as clones whenever the distance between two BrdU-positive nuclei was less than 1.5 times the diameter of the nucleus. As in the rat [18, 19] and as we show here, spermatogonia located at this distance are connected by cytoplasmic bridges. As additional criteria the clones had to show the same or a very similar intensity and pattern of BrdU labeling as this indicates a synchrony of their cell cycle and the distance between two similarly stained nuclei was not more than approximately 1.5 times the diameter of such a nucleus. These criteria were chosen because a similar BrdU staining pattern in various cells indicates that the timing of S-phase in these cells is synchronized. In hematoxylin-stained whole mounts, cytoplasmic bridges (indicating a clonal origin of several cells) between spermatogonia can only be detected in cells not further separated than approximately 1.5 times their nuclear diameter. Using these criteria, the number of clones of BrdU-positive spermatogonia and the number of spermatogonia per clone was determined for stages VII, IX, and XII of the seminiferous epithelium using seminiferous tubules of two adult male rhesus monkeys. The total number of BrdU-labeled spermatogonia was counted for a certain number of sites (a site being an area of a seminiferous tubule fragment showing a given stage of the cycle of the seminiferous epithelium) per stage, and the number of cells of each spermatogonial clone was determined.

RESULTS

Detection of Proliferating Cells in Whole Mounts of Adult Marmoset Seminiferous Tubules

Whole mounts derived from testes removed 3 h after an i.v. bolus injection of BrdU show BrdU-labeled cells forming long chains oriented in longitudinal direction along the tubule (Fig. 1a). These cells are located adjacent to the basement membrane of the tubule. In other areas fields of scattered BrdU-positive cells were observed (Fig. 1, b and c). The sizes of the nuclei differed distinctly between 8 and 12 μm.

Stages of Spermatogenesis and Spermatogonial Clones As Visualized in Whole Mounts of Adult Rhesus Monkey Seminiferous Tubules

The whole mounts consisted of intact seminiferous tubules with diameters of 200–300 μm. In the whole mounts, BrdU-labeled germ cells were easily visualized by our immunohistochemical staining (Fig. 2a). The positive cells were attached to or located close to the basement membrane of the structurally intact seminiferous tubules. The three-dimensional organization becomes obvious using confocal microscopy. Whereas the BrdU-positive germ cells are al-

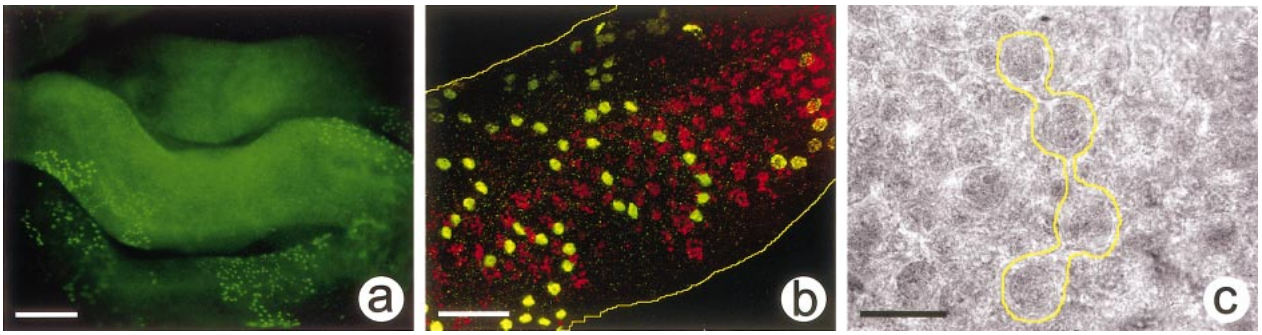

FIG. 2. Fluorescence (**a**), confocal (**b**), and bright field (**c**) micrographs of whole mounts of adult rhesus monkey seminiferous tubules. **a**) Low power fluorescence micrograph showing the immunohistochemical localization of BrdU-positive cells (green) in intact seminiferous tubules. The positive cells are depicted as small or large clusters close to the basement membrane of the seminiferous tubules. Bar = 200 μm. **b**) Confocal microscopy reveals the three-dimensional arrangement of BrdU-positive germ cells (green) and spermatids (acrosin staining [red]) in stage IV of spermatogenesis. The yellow superimposed lines outline the seminiferous tubule. Clones of B_3 spermatogonia are lined up along the basal lamina around the seminiferous tubule. Spermatids are grouped in clusters and are located close to the lumen of the seminiferous tubule. Bar = 50 μm. **c**) High-power bright-field microscopy of hematoxylin-stained whole mount preparations reveals the existence of cytoplasmic bridges between A_{pale} spermatogonial clones at stage VII of spermatogenesis. (To allow easy recognition, the clone has been outlined in bright yellow.) Bar = 25 μm.

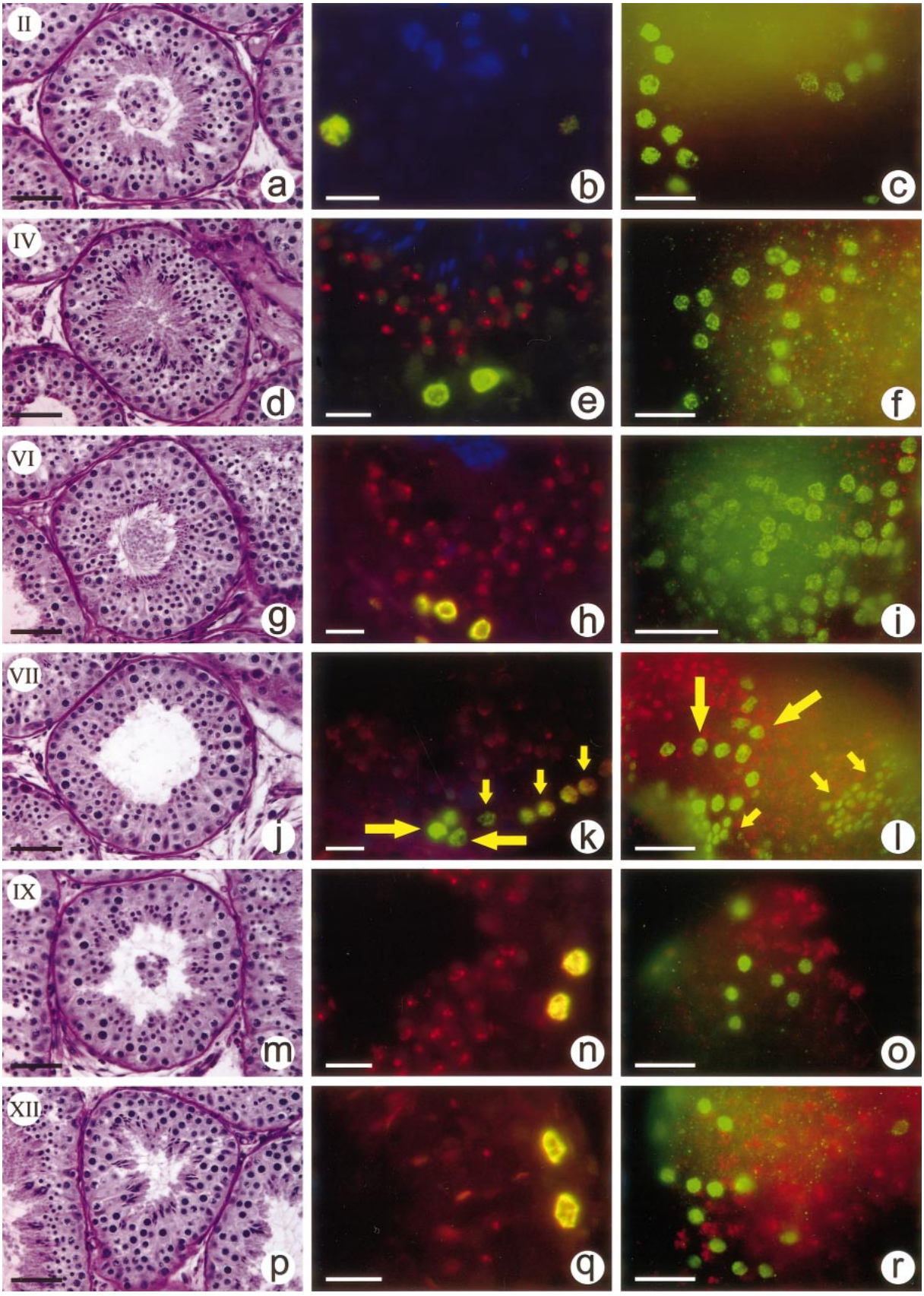

FIG. 3. Micrographs showing different stages of rhesus monkey spermatogenesis. The micrographs are representative examples of the six stages of the seminiferous epithelial cycle when BrdU-positive premeiotic germ cells are present. (The number of the stage shown in each row appears in the upper left corner of each micrograph in the left column.) Column I: Haematoxylin/PAS-stained paraffin-embedded tissue, 5-μm sections. Bar = 50 μm. Column II: Triple-immunofluorescent detection of BrdU (green/yellow), acrosin (red), and DNA (blue) in paraffin-embedded tissue, 5-μm sections. Bar = 15 μm. Column III: Immunofluorescent labeling of BrdU (green/yellow) and acrosin (red) in whole mounts of seminiferous tubules. Bar = 50 μm. **a**–**c**) Stage II of rhesus monkey spermatogenesis (**a**). Strongly DAPI-stained elongated spermatids are present. The acrosomal droplet in round

ways observed in the periphery of the seminiferous tubules, the acrosomal staining of round and elongating spermatids was located close to the lumen of the seminiferous tubules (Fig. 2b). Depending on their variable duration, each stage of the cycle of the seminiferous epithelium extended longitudinally over a distance of 200–800 μm of the seminiferous tubule.

Labeled spermatogonia in all stages of the seminiferous epithelium appear as chains of closely arranged germ cells of identical nuclear size, shape, structure, and staining intensity. In these chains the distance from one nucleus to the other was not wider than the diameter of the nucleus (Fig. 2b). The BrdU-staining intensity and nuclear morphology was similar in all spermatogonia of a single chain but differed considerably between chains even when they were closely arranged, indicating a high degree of cell cycle synchrony in a given chain. Hematoxylin-stained whole mounts revealed that the juxtaposed cells in these chains were connected by cytoplasmic bridges, thus creating a cytoplasmic continuum (Fig. 2c). As the spermatogonia within these chains are closely positioned to one another, are connected via cytoplasmic bridges, and have high synchrony of their cell cycle, we postulate a clonal origin of these chains of spermatogonia. Therefore we will refer to the chains of spermatogonia in the following as ''spermatogonial clones.''

Spermatogonial clones in two adult rhesus monkeys at stages VII, IX and XII of the cycle of the seminiferous epithelium

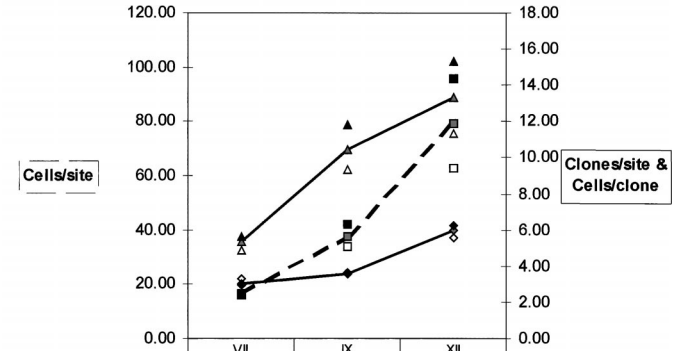

	VII	IX	XII
Cells/site average	16.33	37.55	79.33
Cell/site 3048	16.50	42.20	95.83
Cells/site 3060	16.00	33.67	62.83
Clones/site average	5.37	10.45	13.33
Clones/site 3048	5.61	11.80	15.33
Clones/site 3060	4.89	9.33	11.33
Cells/clone average	3.04	3.59	5.95
Cells/clone 3048	2.94	3.58	6.25
Cells/clone 3060	3.27	3.61	5.54

FIG. 4. BrdU-labeled spermatogonia and their clonal organization at three stages of the seminiferous epithelium of adult male rhesus monkeys.

BrdU-labeled Cells at Different Stages of the Cycle of Spermatogenesis 3 h Post–BrdU Injection

In whole mounts of rhesus monkey seminiferous tubules, which show a longitudinal arrangement of the stages of the cycle of the seminiferous epithelium, the dual label for BrdU and acrosin enabled us to identify cohorts of proliferating spermatogonia and to accurately determine the stage in which these cells are located. We had to define criteria for our staining method in cross-sections and whole mounts to allow a correlation of all stages of spermatogenesis showing BrdU-positive spermatogonia with the conventionally used morphological criteria for the stages of the cycle of the seminiferous epithelium of the rhesus monkey (Fig. 3) [1]. Our criteria are as follows.

Stage II. In stage II of spermatogenesis (Fig. 3a), few labeled B_2 spermatogonia are observed in sections (Fig. 3b). Acrosin is virtually undetectable. Elongated spermatids are present at the luminal surface of the epithelium. In whole mounts, the labeled B_2 spermatogonia are clearly organized as 8- or 16-cell clones, and acrosin staining is not visible (Fig. 3c).

Stage IV. In stage IV of spermatogenesis (Fig. 3, day), numerous labeled B_3 spermatogonia are present in sections (Fig. 3e). The acrosome of the round spermatids visualized by acrosin staining appears as a small pale cap with one brighter spot. Clusters of elongated spermatids are embedded at the luminal surface of the seminiferous epithelium. In whole mounts, a loose network of labeled B_3 spermatogonia is visible. Most of those spermatogonia are apparently organized in clones of 16 or 32 cells. One 16-cell clone is depicted in Figure 3f. The acrosome appears as a small bright dot.

Stage VI. In stage VI of spermatogenesis (Fig. 3g), many labeled B_4 spermatogonia are present (Fig. 3h). Acrosomal caps as visualized by acrosin extend over one third of the round spermatids and show bright tips. The caps are randomly oriented and do not uniformly point to the outer wall of the seminiferous tubule. Elongated spermatids are present at the luminal surface of the seminiferous epithelium. In whole mounts, the labeled B_4 spermatogonia appear as a dense network (Fig. 3i). Distinction between individual clones is no longer possible because of the close proximity of each clone to adjacent clones. The acrosome appears as bright spots.

Stage VII. In stage VII of spermatogenesis (Fig. 3j), two types of BrdU-labeled cells appear in the sections, few A_{pale}

spermatids is extremely small and barely visible. The BrdU-positive B_2 spermatogonia are often seen as single cells or pairs in cross-sections (**b**). Whole mount showing B_2 spermatogonia organized as an eight-cell clone (**c**). **d**–**f**) Stage IV of rhesus monkey spermatogenesis (**d**). Strongly DAPI-stained elongated spermatids are present. The acrosomal droplet in round spermatids is now clearly visible. The BrdU-positive B_3 spermatogonia are often seen as single cells or pairs in cross-sections (**e**). Whole mount showing B_3 spermatogonia organized as 16-cell-clone (**f**). **g**–**i**) Stage VI of rhesus monkey spermatogenesis (**g**). Strongly DAPI-stained elongated spermatids are lined up close to the lumen of the tubules. The acrosome is an irregular droplet with protrusions beginning to form a cap on round spermatids. Several BrdU-positive B_4 spermatogonia are seen in each tubule cross-section along the basement membrane (**h**). B_4 spermatogonial clones can be detected forming large networks (**i**). **j**–**l**) Stage VII of rhesus monkey spermatogenesis (**j**). No elongated spermatids are present. The acrosome is forming a cap on round spermatids. Numerous BrdU-positive preleptotene spermatocytes (small arrows) are seen in each tubule cross-section as a layer of germ cells slightly detached from the basement membrane. In some areas, BrdU-positive A_{pale} spermatogonia are observed adjacent to the basal lamina (**k**, big arrows). The large number of small preleptotene spermatocytes form a dense network of BrdU-positive cells in whole mounts (small arrows). The larger BrdU-positive A_{pale} spermatogonia (big arrows) can typically be seen as four-cell clones in whole mount preparations (**l**). **m**–**o**) Stage IX of rhesus monkey spermatogenesis (**m**). No elongated spermatids are present. The acrosome is forming an irregular cap on the early elongating spermatids. BrdU-positive A_{pale} spermatogonia are observed adjacent to the basal lamina (**n**). BrdU-positive A_{pale} spermatogonia are typically forming four-cell clones in whole mount preparations (**o**). **p**–**r**) Stage XII of rhesus monkey spermatogenesis (**p**). No elongated spermatids are present. The acrosome forms a V-shaped irregular cap on elongating spermatids. BrdU-positive B_1 spermatogonia are seen adjacent to the basal lamina (**q**). B_1 spermatogonia are mostly encountered as four- or eight-cell clones in whole mounts (**r**).

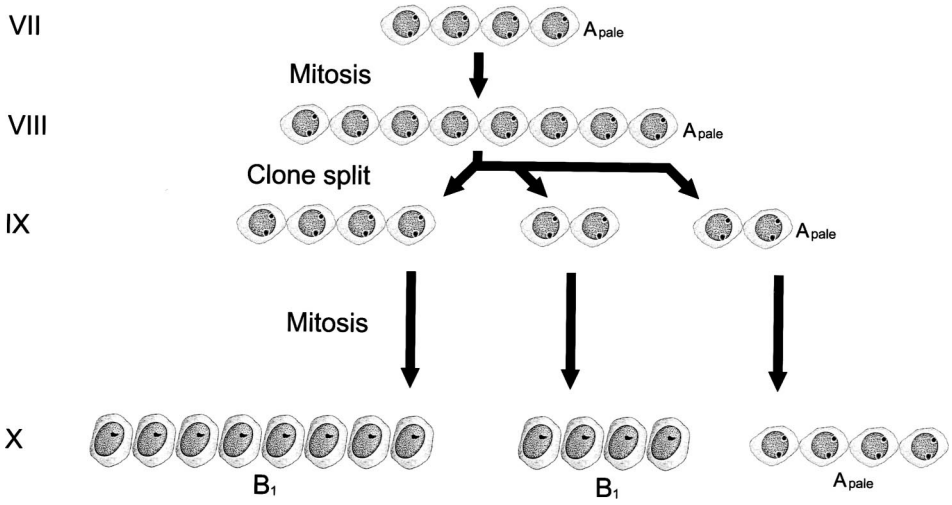

FIG. 5. Expansion of spermatogonial clones in adult male rhesus monkeys from stages VII to X of spermatogenesis taking a four-cell clone of A_{pale} spermatogonia as the starting point.

spermatogonia in mitotic S-phase and a large number of preleptotene spermatocytes in S-phase before meiosis (Fig. 3k). The acrosin staining reveals an acrosomal cap that extends over half of each round spermatid, with the tip of the acrosome being uniformly oriented toward the outer wall of the seminiferous tubule. Elongated spermatids are absent. In whole mounts, the labeled A_{pale} spermatogonia appear to be organized as two- or four-cell clones (Fig. 3l). Labeled preleptotene spermatocytes are present throughout most of the seminiferous epithelium at this stage of spermatogenesis. Acrosin staining shows the cap-shaped acrosome of the round spermatids.

Stage IX. In stage IX of spermatogenesis (Fig. 3m), few labeled A_{pale} spermatogonia are present in the sections (Fig. 3n). The acrosin staining depicts the V-shaped acrosomal caps of elongating spermatids. In whole mounts, the labeled A_{pale} spermatogonia are organized in two- or four-cell clones (Fig. 3o).

Stage XII. In stage XII of spermatogenesis (Fig. 3p), few labeled B_1 spermatogonia are present (Fig. 3q). The acrosin staining clearly visualizes the narrow V-shape of the elongating spermatids. Elongated spermatids are absent. In whole mounts, the labeled B_1 spermatogonia appear to be arranged as four- or eight-cell clones (Fig. 3r).

Spermatogonial Clones

The number of BrdU-labeled spermatogonia, the number of BrdU-positive spermatogonial clones, and the number of spermatogonia per clone were determined quantitatively for stages VII, IX, and XII of the seminiferous epithelium in whole mount preparations of two adult male rhesus monkeys (Fig. 4). For stage VII, 27 sites containing a total of 441 A_{pale} spermatogonia organized in 145 clones were evaluated. For stage IX, 11 sites containing a total of 413 A_{pale} spermatogonia organized in 115 clones were evaluated. For stage XII, 12 sites containing a total of 952 B_1 spermatogonia organized in 160 clones were evaluated. The average number of labeled cells per site doubled from 16.3 in stage VII to 37.6 in stage IX and approximately doubled once more to 79.3 in stage XII. The average number of clones per site also doubled from 5.4 in stage VII to 10.5 in stage IX, but increased only slightly to 13.3 in stage XII. Consequently, the average number of cells per clone increased only slightly from 3.0 in stage VII to 3.6 in stage IX, but nearly doubled to 6.0 in stage XII (Fig. 4).

DISCUSSION

Spermatogenesis in non-human primates has been extensively studied in the past [1–6]. Several types of spermatogonia have been described and a series of models explaining the kinetics of spermatogonial expansion have been postulated [8]. However, some controversy persists on this topic, and none of the previous investigations has presented an in-depth evaluation of the long-proposed [1, 2, 13] clonal organization of spermatogonial stem cells at different stages of spermatogenesis.

Using a new approach, we first encountered clones of proliferating spermatogonia in the marmoset (*C. jacchus*). The seminiferous epithelium in this species resembles the arrangement of the stages of spermatogenesis in the human seminiferous epithelium as several stages are found per tubular cross-section and the stages are not longitudinally separated along the seminiferous tubules [20]. The complex organization made it difficult to establish a strong correlation between spermatogonial clones and specific stages of spermatogenesis. More accessible models for studying the clonal expansion in non-human primates are members of the old-world primate family *Cercopithecidae*, since all species of macaques studied so far show a longitudinal separation of the stages of spermatogenesis along the seminiferous tubules. The most commonly used criteria for staging (12 stages of the seminiferous epithelium) were established by Clermont and Leblond [1] using the rhesus monkey (*M. mulatta*), Clermont [2] using the vervet monkey (*Cercopithecus aethiops*), and Clermont and Antar [3] using the stump-tailed macaque (*Macaca arctoides*). Other research groups have used identical criteria for the crab-eating macaque (*Macaca fascicularis*) [6].

A_{pale} Spermatogonial Self-replenishing Division

A_{dark} spermatogonia were repeatedly shown to have a very low proliferation rate in healthy adult non-human primates and are therefore considered proliferatively inactive reserve stem cells [3, 5]. The cycling A spermatogonium is the A_{pale}. Controversy persists to date whether one or two divisions of A_{pale} spermatogonia occur in macaque testes during the initial phase of spermatogenesis. Whereas a single division of A_{pale} spermatogonia for the rhesus monkey and the vervet monkey was postulated to occur at stages IX–X, two divisions have been described for the stump-tailed macaque occurring at stages VII and IX [1, 3, 8]. The

first division of A_{pale} spermatogonia at stage VII is a self-replenishing division of A_{pale} spermatogonia as their numbers increase but no B spermatogonia are formed. Here we present unequivocal evidence for the existence of two divisions of A_{pale} spermatogonia also in the rhesus monkey occurring at stages VII and IX of spermatogenesis. Several reasons might explain why the first division of A_{pale} spermatogonia has not been detected in previous studies. These earlier studies used tissue sections, and their analytical strategies relied on approaches using either 1) counts of colchicine-blocked mitotic metaphases [1] or 2) incorporation of tritiated thymidine and subsequent qualitative and quantitative analysis of radiographs for detection of cells in the S-phase of the cell cycle [2, 3]. For the former, the mitoses of A_{pale} spermatogonia at stage VII of the cycle of the rhesus monkey have apparently been missed due to their very low numbers (see discussion in [2]). For the latter, studying spermatogenesis in *C. aethiops*, it is not unlikely that the radioactivity emitted from the small number of A_{pale} spermatogonia going through S-phase at stage VII is masked by the high radiation emission from a much larger number of preleptotene spermatocytes going through S-phase before meiosis at the same stage of spermatogenesis. Indeed we obtained the first and most obvious evidence of a first division of A_{pale} spermatogonia at stage VII by analysis of whole mounts. We observed that at stage VII of the cycle of the seminiferous epithelium of the rhesus monkey, in addition to BrdU-labeled preleptotene spermatocytes, duplets and quadruplets of BrdU-positive cells are present with significantly bigger nuclei than the preleptotene spermatocytes. Comparing the size and location of those BrdU-labeled cells with the position and appearance of A_{pale} spermatogonia in conventionally stained sections and whole mounts, we confirmed that these BrdU-positive cells are A_{pale} spermatogonia. Our data reveal that spermatogenesis in the rhesus monkey is initiated with a division of A_{pale} spermatogonia at stage VII of spermatogenesis as in other old world monkeys of the family Cercopithecidae, thus rendering the concept of interspecific differences obsolete.

Spermatogonial Division Modalities and Clonal Size

Spermatogonia in the mammalian testis must 1) maintain their own population and 2) give rise to differentiating cells. Much effort has been spent over several decades to describe the kinetics of this process. More than 60 yr ago, Rolshoven [21] proposed the concept of a so-called differential mitosis. He stated that an unequal spermatogonial mitosis gives rise to one spermatogonium and one spermatocyte. Many subsequent studies [1–3, 8, 14, 22] have addressed this question, but in none of these studies the existence of an unequal mitosis has been proven. For nonhuman primates it can be concluded that although the A_{pale} spermatogonial population gives rise to both new A_{pale} spermatogonia and to B_1 spermatogonia, no individual mitotic division of an A_{pale} spermatogonium will result in a different kind of progeny, becoming a mixed pair of an A_{pale} and B_1 spermatogonium. Every spermatogonial division always produces two identical daughter cells [1–3, 8]. Looking more into the details of the generation of different types of daughter cells, it becomes obvious that the first division of A_{pale} spermatogonia occurs already from pairs of cells. These pairs have been described to be of clonal origin as they are connected by cytoplasmic bridges [18, 19, 23, 24]. Clermont and Leblond [1] described A_{pale} spermatogonia in the rhesus monkey to be at all stages organized in pairs or quadruplets, which strongly supports the fact that the starting point of spermatogenesis is the synchronized division of a pair or quadruplet of A_{pale} spermatogonia. Using the whole mount approach, we demonstrate here that 1) the total number of labeled spermatogonia doubles from stages VII to IX and again from stages IX to stage XII; and 2) proliferating A_{pale} spermatogonia at stages VII and IX of spermatogenesis are always encountered at least as pairs, but more frequently as quadruplets; and c) B_1 spermatogonia are encountered forming clones of four or eight cells. Although no detailed analysis of the sizes of B_2-, B_3-, and B_4 spermatogonia could be made due to the close juxtaposition of several clones and the resulting difficulties in differing between one clone and the next, the clones appeared to become larger after each mitotic division. Based on our findings (Fig. 4), we propose the following model (Fig. 5): A_{pale} spermatogonia at stage VII of spermatogenesis are organized as functional units of pairs or quadruplets. Most if not all A_{pale} spermatogonia proliferate at stage VII/VIII, resulting in a doubling of the A_{pale} population at stage VIII/IX. The quadruplets or eight-cell clones of A_{pale} spermatogonia resulting from the first mitosis are unstable and separate into pairs or quadruplets of A_{pale} spermatogonia. This explains the doubling of spermatogonial numbers and clones while having a stable number of A_{pale} spermatogonia in each clone. At stage IX the separated clones enter a next mitosis, giving rise to either eight B_1 spermatogonia, or separate further into two pairs, giving rise to one quadruplet of A_{pale} spermatogonia and one quadruplet of B1 spermatogonia (Fig. 5). Whereas the four-cell clone of A_{pale} spermatogonia remains mitotically quiescent until the next stage VII, replenishing the original A_{pale} population for this cycle of spermatogenesis, the B_1 clones enter the subsequent differentiation steps and mitotically divide into B_2 spermatogonia, thus forming always bigger clones after each further B spermatogonial division. Theoretically, 16-cell clones of B_2-, 32-cell clones of B_3-, 64-cell clones of B_4 spermatogonia, and thus 128-cell clones of spermatocytes can be expected following our model, which is in accordance with our qualitative observations. Often the starting point appears not to be a four-cell clone, but a pair of A_{pale} spermatogonia at stage VII of the cycle. Then the numbers of the differentiating germ cells are only half of those stated in the first example. Our data reveal a mixture of two- and four-cell clones at stage VII.

Our model (Fig. 5) is identical with the second of the two proposed models by Clermont and Antar [3]. They presented these two models because from their own data they could not unequivocally determine the correct kinetics of premeiotic germ cell expansion. In the light of our data, we conclude that their model 2 is correct as it is supported by our data presented in Figure 5. In addition to their previous findings, we add the clonal modalities of spermatogonial expansion, thus rendering the model more acceptable. Although our proposed model is in accordance with our novel findings as well as the previously published data [3], further studies are needed to unequivocally confirm the modalities of the clonal expansion in the monkey testis.

ACKNOWLEDGMENTS

We gratefully acknowledge the testicular tissue and tissue sections that were provided to us by Dr. Tony M. Plant (University of Pittsburgh, School of Medicine, Department of Cell Biology and Physiology) and that were derived from work that was supported by NICHD/NIH through a cooperative agreement (U54-HD-08610) as part of the Specialized Coop-

erative Centers Program in Reproduction Research. We thank Dr. Simon Watkins and his coworkers (University of Pittsburgh, School of Medicine, Department of Cell Biology and Physiology) for providing us with excellent imaging facilities, and Dr. David R. Simorangkir (University of Pittsburgh, School of Medicine, Department of Cell Biology and Physiology) for kindly providing support during preparations of the tissues.

REFERENCES

1. Clermont Y, Leblond CP. Differentiation and renewal of spermatogonia in the monkey, *Macacus rhesus*. Am J Anat 1959; 104:237–273.
2. Clermont Y. Two classes of spermatogonial stem cells in the monkey (*Cercopithecus aethiops*). Am J Anat 1969; 126:57–71.
3. Clermont Y, Antar M. Duration of the cycle of the seminiferous epithelium and the spermatogonial renewal in the monkey *Macaca arctoides*. Am J Anat 1973; 136:153–165.
4. Kluin PM, Kramer MF, de Rooij DG. Testicular development in *Macaca irus* after birth. Int J Androl 1983; 6:25–43.
5. Fouquet JP, Dadoune JO. Renewal of spermatogonia in the monkey (*Macaca fascicularis*). Biol Reprod 1986; 35:199–207.
6. Zhengwei Y, McLachlan RI, Bremner WJ, Wreford NG. Quantitative (stereological) study of the normal spermatogenesis in the adult monkey (*Macaca fascicularis*). J Androl 1997; 18:681–687.
7. Dym M, Clermont Y. Role of spermatogonia in the repair of the seminiferous epithelium following x-irradiation of the rat testis. Am J Anat 1970; 128:265–282.
8. Clermont Y. Kinetics of spermatogenesis in mammals: seminiferous epithelium cycle and spermatogonial renewal. Physiol Rev 1972; 52: 198–236.
9. Bellve AR, Cavicchia JC, Millette CF, O'Brian DA, Bhatnagar YM, Dym M. Spermatogenic cells of the prepuberal mouse. Isolation and morphological characterization. J Cell Biol 1977; 74:68–85.
10. de Rooij DG, van Alphen MM, van de Kant HJ. Duration of the cycle of the seminiferous epithelium and its stages in the rhesus monkey (*Macaca mulatta*). Biol Reprod 1986; 35:587–591.
11. van Alphen MM, de Rooij DG. Depletion of the seminiferous epithelium of the rhesus monkey, *Macaca mulatta*, after X-irradiation. Br J Cancer Suppl 1986; 7:102–104.
12. van Alphen MM, van de Kant HJ, de Rooij DG. Depletion of the spermatogonia from the seminiferous epithelium of the rhesus monkey after X irradiation. Radiat Res 1988; 113:473–486.
13. van Alphen MM, van de Kant HJ, de Rooij DG. Repopulation of the seminiferous epithelium of the rhesus monkey after X irradiation. Radiat Res 1988; 113:487–500.
14. De Rooij DG, van Dissel-Emiliani FM, van Pelt AM. Regulation of spermatogonial proliferation. Ann N Y Acad Sci 1989; 564:140–153.
15. Rosiepen G, Arslan M, Clemen G, Nieschlag E, Weinbauer GF. Estimation of the duration of the cycle of the seminiferous epithelium in the non-human primate *Macaca mulatta* using the 5-bromodeoxyuridine technique. Cell Tissue Res 1997; 288:365–369.
16. Wistuba J, Schrod A, Greve B, Hodges JK, Aslam H, Weinbauer GF, Luetjens CM. Organization of seminiferous epithelium in primates: relationship to spermatogenic efficiency, phylogeny, and mating system. Biol Reprod 2003; 69:582–591.
17. Ramaswamy S, Marshall GR, Pohl CR, Friedman RL, Plant TM. Inhibitory and stimulatory regulation of testicular inhibin B secretion by luteinizing hormone and follicle-stimulating hormone, respectively, in the rhesus monkey (*Macaca mulatta*). Endocrinology 2003; 144: 1175–1185.
18. Huckins C, Oakberg EF. Morphological and quantitative analysis of spermatogonia in mouse testes using whole mounted seminiferous tubules: the normal testis. Anat Rec 1978; 192:519–528.
19. Huckins C. Spermatogonial intercellular bridges in whole mounted seminiferous tubules from normal and irradiated rodent testes. Am J Anat 1978; 153:97–122.
20. Millar MR, Sharpe RM, Weinbauer GF, Fraser HM, Saunders PT. Marmoset spermatogenesis: organizational similarities to the human. Int J Androl 2000; 23:266–277.
21. Rolshoven E. Zur Frage des ''Alterns'' der generativen Elemenete in den Hodenkanälchen. Anat Anz 1941; 91:1–8.
22. Plant TM, Marshall GR. The functional significance of FSH in spermatogenesis and the control of its secretion in male primates. Endocr Rev 2001; 22:764–786.
23. Gondos B, Zemjanis R. Fine structure of the spermatogonia and intercellular bridges in *Macaca nemestrina*. J Morphol 1970; 131:431–446.
24. Dym M, Fawcett DW. Further observations on the numbers of spermatogonia, spermatocytes, and spermatids connected by intercellular bridges in the mammalian testis. Biol Reprod 1971; 4:195–215.